BIW10 Preprint -- Edited; preliminary green dot status
Final version will appear on JACoW

SIMULATION OF A CAVITY BPM FOR HIGH RESOLUTION SINGLE-PASS BEAM POSITION MEASUREMENTS

A. Morgan, G. Rehm, Diamond Light Source, UK
A. Lyapin, University College London , UK
S. Boogert, N. Joshi, S. Molloy, Royal Holloway University London, UK

Abstract

This paper describes the design of a cavity BPM for use in single pass machines. The design was modelled using a number of different EM codes to allow cross comparison of the simulation results. Furthermore, in addition to existing designs, the geometry has been modified to introduce a frequency separation between the horizontal and vertical dipole signals, as well as a reduction of the sensitivity of the position monitor to the monopole sum signal. The next stage of this project will be the manufacture of a prototype for tests in the transfer path at Diamond Light Source.

DESIGN REQUIREMENTS

Modern and future single-pass machines such as Free Electron Lasers and Linear Colliders require fast and sensitive beam position monitors (BPMs) able to do precision beam position measurements of individual bunches.

Cavity BPMs have been shown to provide nanometre level resolutions [1], while stability studies resulted in micrometre and even sub-micrometre drifts over a few hours [2].

Several methods of improving the time resolution of cavity BPMs allow for bunches separated by 10s of nanoseconds to be resolved.

Basing on the previous works we wanted to take advantage of the simple cylindrical geometry and the inherent filtering effects of the slot-coupled design in order to better select out the desired dipole mode, while simultaneously suppressing the signals from the unwanted modes.

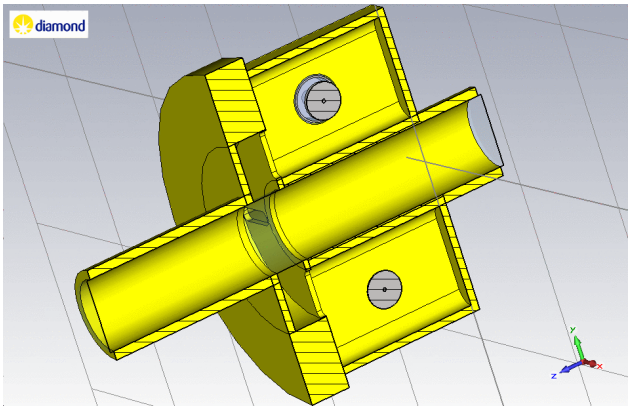

Figure 1: Full cavity BPM geometry

We also aim at simplifying the design flow, making the BPM easy and hence inexpensive to manufacture, and also fixing the remaining problems of cavity BPMs, such as the cross-coupling of the horizontal and the vertical signals.

As with many other recent cavity BPMs[3,4,5], this design comprises of a resonant cavity with coupling slots leading into waveguides. Each waveguide has a pickup in it to transmit the signal down a coaxial line for signal processing. (See figure 1)

Resonant cavity

The radius of the resonant cavity is determined by the frequency we are interested in. In the longer term we want to use the Diamond RF system (running at 499.654 MHz) to deliver local oscillator (LO) signals for down conversion. We chose the 13th harmonic, which gave us an initial target of 6.495 GHz. The dipole mode frequency has to be slightly offset from the peak so once the signal is down converted it sits near the centre of the IF bandwidth. A 100Msample ADC gives 50MHz bandwidth so a 20 MHz offset downwards was included, bringing the target to 6.475 GHz.

The longer the cavity the stronger it couples to the beam. On the other hand, the cavity becomes sensitive to the beam incline while the sensitivity increase with the length drops due to the signal in the cavity and the beam becoming asynchronous. 8 mm length was found to provide enough coupling while keeping the timing effects to a minimum.

Waveguide

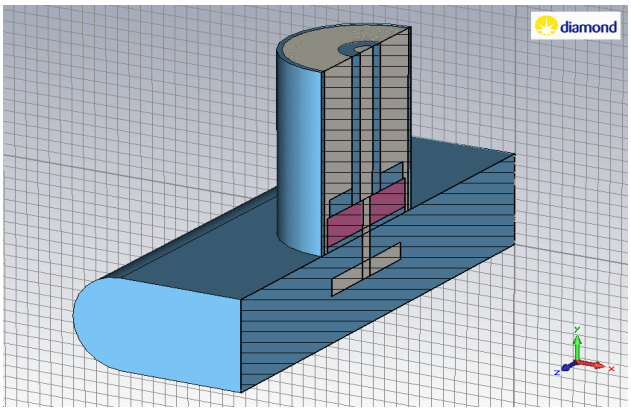

Figure 2: waveguide and coaxial port geometry

The dimensions of the waveguides are such that the first monopole mode is below the waveguide cut-off for the lowest odd mode TE_{01}, so that the monopole mode signal leaking due to asymmetries is suppressed, while the dipole mode is the first mode transmitted by the TE_{01}.

Although the other modes can be present near the slots they do not propagate. Therefore the length of the

waveguide can determine the amount of filtering seen by unwanted modes coupled through the slots.

The location of the coaxial port on the waveguide, and the location of the coupling plate in the waveguide is such to maximise the coupling from waveguide to coaxial modes.

Coupling slots

The width of the coupling slots in the two planes is different (4mm for x and 3mm for y).

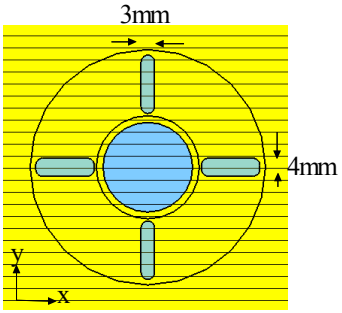

Figure 3: Coupling slot geometry

This achieves some frequency separation between the horizontal and vertical polarisations of the dipole mode which allows us to improve the rejection of the cross coupled signal once the signal is digitised.

This is because we do digital down conversion using different frequencies for x and y. The signals are then passed through a filter with a passband small enough that the cross-coupled signals fall outside and so are suppressed .

CODE COMPARISONS

Several different EM modelling codes were used in parallel for this design (CST studio, GdfidL[6], Omega3P). This gave us an idea of the amount of confidence we should give to a particular result. Once all three codes converged we could be sure we had a representative result.

In order to find out the different codes' strengths and weaknesses, some simpler simulations were done. The idea of this was to get an understanding of the mesh densities required to get good results for the cylindrical geometry using cartesian geometry codes. This is because once the details of the full design are added, radial symmetry is broken and you need a cartesian model to fully represent the desired geometry.

Pillbox cavity

The first was a simple pill box cavity of the dimensions of the main resonance cavity of the CBPM. This allowed us to not only compare the codes against each other, but also with the theoretical predictions for this geometry.

The theoretical frequency results were generated from this analytical formula[7].

$$f_{(mnp)} = \frac{c}{2\pi}\sqrt{\left(\frac{j_{mn}}{b}\right)^2 + \left(\frac{p\pi}{l}\right)^2}$$

Where f is the frequency and j are zeros of the bessel function J_m in a cylindrical coordinate system, while b and l are the radius and length of the cavity respectively. Under the assumption of no modes in the z direction p is always 0. Also we are mainly interested the lowest radial mode, so n is always 1. So the frequencies of the monopole, dipole and quadrupole modes are where j_{nm} is j_{01}, j_{11} and j_{21} respectively.

In order to find the theoretical Q values, we first needed to calculate the skin depth, using

$$\delta = \frac{1}{\sqrt{\pi \sigma \mu f}}$$

which we can then use with

$$Q = \frac{1}{\delta}\frac{l}{1+\frac{l}{b}}$$

Where b and l have the same meaning as before. f is the frequency of interest, μ is the magnetic permeability of the cavity wall material, while σ is the electrical conductivity of the cavity material.

To within 2.3MHz all the codes agree with the theoretical expectation of the frequency (Table 1). The spread of results between the codes is also of the same order, with the monopole mode having the closest agreement and the quadrupole mode diverging the most.

The increasing divergence between the codes as you move from monopole to dipole to quadrupole is due to the fact that the mesh is unable to describe the higher frequency modes as accurately .

Table 1:Eigenmode frequency results for the pillbox.

Pill box cavity (Frequencies (GHz))					
		Difference from theory (MHz)			
Mode	Theory	CST	GdfidL	Omega 3P	Spread (MHz)
Monopole	4.3414	-0.2	0.0	1.0	1.2
Dipole	6.9173	-0.5	0.0	1.6	2.1
Quadrupole	9.2712	-1.2	1.1	2.3	3.5

The Q factors also agree well with the theoretical prediction (see table 2).

Table 2:Eigenmode Q_0 results for the pillbox.

Pill box cavity (Q factors)					
		Difference from theory			
Mode	Theory	CST	GdfidL	Omega 3P	Spread
Monopole	6123	0	55	-7	62
Dipole	7729	2	75	-15	90
Quadrupole	8948	2	55	-24	79

Pillbox cavity with beam pipe

The next step was to do the same analysis on a pillbox cavity on a beam pipe. Again, with the same dimensions as the full design.

Again the codes showed good agreement on the frequencies with the dipole being within 3MHz (see table3).

Table 3: Frequency results for pillbox on beam pipe

Pill box cavity with beam pipe (Frequencies (GHz))				
Mode	CST	GdfidL	Omega3P	Spread (MHz)
Monopole	4.7071	4.7111	4.7030	8.1
Dipole	6.4750	6.4764	6.4734	3
Quadrupole	9.0025	9.0030	9.0045	2

The Q values broadly agreed but the reduced ability of the mesh to describe the higher frequency modes is more pronounced (see table 4).

Table 4:Eigenmode Q_0 results for pillbox on beam pipe.

Pill box cavity with beam pipe (Q factors)				
Mode	CST	GdfidL	Omega3P	Spread
Monopole	6272	6373	6266	107
Dipole	7144	7612	7687	543
Quadrupole	8425	9864	9077	1439

These studies allowed us to develop an understanding of the limits of the codes and to spot indicators of poor convergence which was vital when dealing with the more complex cavity BPM model.

RESULTS FOR THE CBPM MODEL

For reasons of computational time and memory, the coaxial pick-ups were omitted from the model.

S parameter results

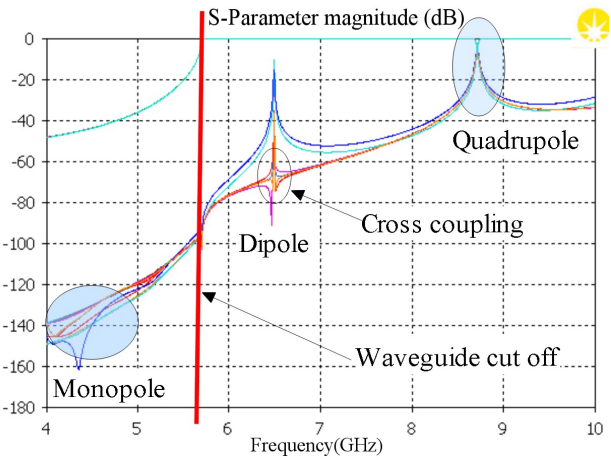

Figure 4: S-parameter response of CBPM

Figure 4 shows a typical S parameter response for the CBPM model.

It can be clearly seen that the residual monopole mode signal is suppressed because it is below the waveguide cut off frequency. Strong resonances can be seen at the dipole and quadrupole frequencies, with the dipole signal being split into coupling in the same plane, and cross coupling between x and y.

Figure 5 shows the ~5MHz frequency separation we get by using the different coupling slot widths for x and y, as described earlier. The blue curves show the transmission from one port to it's pair on the same axis. All the other curves are cross coupling terms and their absolute values are largely determined by the mesh density of the model.

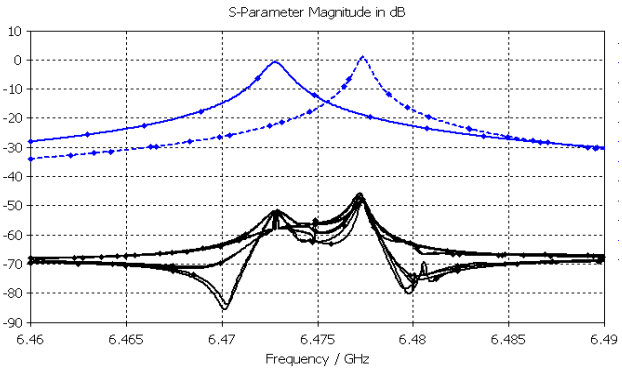

Figure 5: S-parameter response of the dipole mode

As expected, the transmission curves have one well defined peak corresponding to the geometry of the coupling slots in each plane. The cross terms show both peaks as the signals are always passing through one of each type of coupling slot.

Wakefield results

Using a wakefield solver has enabled us to simulate the cavity's response to an excitation with a charged particle bunch travelling through the beam pipe, as compared to the excitation on the ports as used in the S-parameter simulation.

By doing both lossless and lossy simulations we could retrieve both the external and loaded Q values.

Both CST and GdfidL were used for the lossless simulations to check for consistency of the results. Both codes gave very similar results, giving us confidence that they are accurate.

The beam simulated was a 3mm long gaussian pulse containing 1nC of charge. By moving the position of the beam in the beam pipe we could determine the effect of an asymmetric input on the structure. The centred position was used to judge what level of signal could be attributed to meshing artefacts.

Figure 6 shows the typical signal coming out of one of the ports, with a 1mm beam offset in both x and y. It is clear that the signals are comprised by different modes with different amplitudes, decaying at different rates.

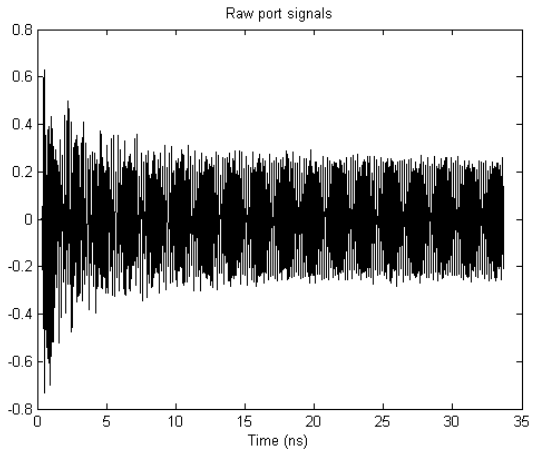

Figure 6: Raw port signals

Indeed, taking the FFT of the port signals we can see that two modes dominate the output (figure 7). For all offsets the dominant mode frequency was 6.47GHz, corresponding to the lowest order dipole mode.

When beam was only offset in either x or y it was the only significant signal. However, when the beam was off axis in both dimensions then an additional peak at 8.85GHz appeared.

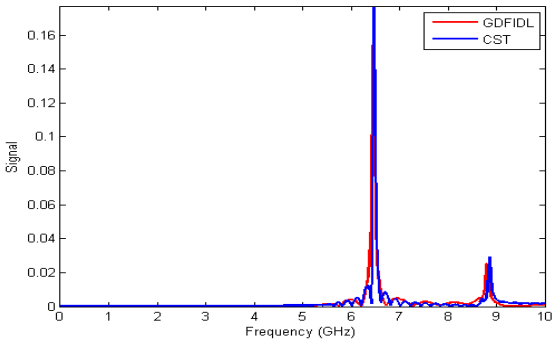

Figure 7: FFT of the port signals

This behaviour is a signature of the quadrupole mode: a beam offset in x or y only produces a field that is symmetric with respect to the slots, and so does not couple into the waveguide. However, when the beam is offset in both x and y, the symmetry gets broken, and the quadrupole mode is generated, some of which is able to couple out into the waveguide. The maximum coupling is achieved when when the beam is equally offset in x and y, so the field is antisymmetric with respect to the slots.

Knowing the peak frequencies in the signal's spectrum, it is possible to demodulate the port signals to find the time domain magnitude evolution of the two modes. Figure 8 shows the decay of the dipole mode (shown in black) and the quadrupole mode (shown in blue) for all 4 output ports. The split between the dipole traces is due to the asymmetry in the coupling slots, the wider slots providing lower external quality factor and shorter decay time.

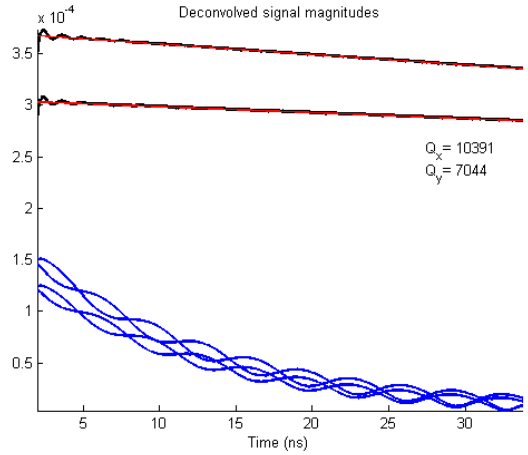

Figure 8: demodulated output signals

From figure 8 it can be seen that the quadrupole component contributes a ~30% early, short term enhancement of the output signals, which can explain the initial shape of the trace seen in figure 6.

By taking the gradient of the initial part of the dipole curve the Q factor can be extracted. Depending on whether material losses are applied to the model this give us either the external or the loaded Q.

The external Q values were ~10,000 and ~7,000 for x and y respectively, while the loaded Q values were ~4,000 and ~3,500 for x and y respectively.

From the loaded Q values we obtained ring down times to 1/e of 0.63us in x, and 0.55us in y. Assuming we want the residual signal to be no more than 5% of the original, this implies 3 ring down periods giving us a maximum bunch repetition frequency of ~500KHz. Of course, by accepting a larger residual signal we could increase the repetition frequency. This is largely determined by the accuracy of the signal subtraction in the digital processing.

By taking the output power integrated over the port geometry, and assuming perfect conversion from waveguide to coaxial transmission the expected signal seen on the 50Ω transmission line can be deduced.

Figure 9 shows the amplitude of the output signal for a 1 mm offset in only one plane. One can see a short pulse peaking to just under 4V and a much slower signal at around 1.3V. The initial pulse is a combination of the signals of all short-live modes that are above the beam pipe cut-off frequency, such as higher order dipole modes etc. These modes decay very quickly as the energy escapes through the beam pipe. Although the pulse looks high compared to the dipole slower decaying signal of the first dipole mode, it can be reduced by orders of magnitude by a band-pass filter in the front-end of the processing electronics.

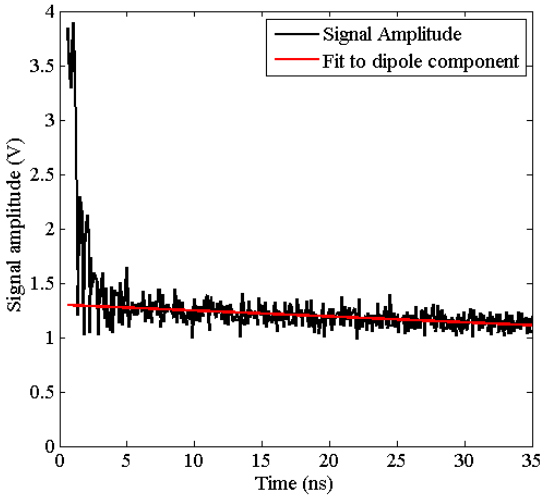

Figure 9: Calculated output signal for 1mm offset

Due to the high Q factor the peak signal for the dipole mode is relatively low, but the energy is spread out over a longer time and in a narrow frequency band. This allows us to use narrow-band filters on the signal in order to get better discrimination between the wanted position signal and the unwanted signals from cross coupling, other cavity modes, and noise. Furthermore, a longer piece of the waveform (compared to the low-Q case) fits into the dynamic range of the electronics and digitisers, and so can be used for digital down-conversion or even fitting analysis.

Consistency check

By using the results of different simulations to get internal Q, the external Q, and the loaded Q (Q_0 ,Q_{ext} and Q_L respectively). A cross check can be done by combining Q_0, Q_{ext} in order to predict Q_L. This value can then be compared against the value for Q_L taken from the wakefield simulation with material losses included.

The Q values are combined in the following way.

$$\frac{1}{Q_L} = \frac{1}{Q_0} + \frac{1}{Q_{ext}}$$

Where Q_0 is the eigenmode result, which include cavity losses. Q_{ext} is the wakefield result with no losses, while Q_L is the wakefield result including losses.

The predicted results show good agreement with the simulated values. The remaining discrepancy can be explained by the fact that the predictions do not take into account any losses of the parts of the structure not covered by the eigenmode models.

Table 5: Comparison of Q values

	Q_0	Q_{ext}	Predicted Q_L	Simulated Q_L	Difference
Using the pillbox with beam pipe eigenmode result					
Q_x	7144	10391	4233	4071	4%
Q_y	7144	7044	3547	3439	3%

SUMMARY

Our design uses proved to work cylindrical cavity with four waveguides coupled via slots for monopole mode reduction. We introduced a frequency split for the two polarisations of the dipole mode making the slots in x and y different. We hope that the isolation between the x and y couplers we observe in the simulations will be confirmed on the prototypes that will be manufactured in the late 2010.

For benchmarking purposes we compared three different EM simulation codes; CST, GdfidL and Omega3P, all of which showed very good agreement between each other and the theory.

The key values we obtained from the simulations include the external Q values: ~10,000 and ~ 7,000 for the x and y axis respectively; and the loaded Q-values of 4071 and 3543. A cross check with internal Q factors showed a the correct relationship with an error less than 5%.

At a bunch repetition frequency of 500kHz the bunch to bunch signal spillover is about 5%, which is low enough for most cases. Much lower spillover can be achieved by subtraction of the digitised signals.

The wakefield simulation gave us an estimate of the output signal of 1.3V for the dipole mode at 1 mm beam offset for a 1 nC bunch charge. An additional short-lived signal initially peaking to 4V was also observed, which, although, is produced by higher order modes and is expected to be strongly suppressed in the electronics.

We are planning to build and test a few prototype cavities in a transfer line of the Diamond light source. We are also looking into involving industrial partners in the manufacturing process, so that if any demand arises for a large scale project, this design can be mass-produced on demand.

REFERENCES

[1] S. Walston et al., Performance of a high resolution cavity beam position monitor system, Nuclear Instruments and Methods, 2007, 10.1016/j.nima.2007.04.162

[2] M. Slater et al., Cavity BPM system tests for the ILC energy spectrometer, Nuclear instruments and Methods, 2008, 10.1016/j.nima.2008.04.033

[3] D. Lipka et. al. Orthogonal coupling in cavity BPM with slots, Proceedings of DIPAC 09, p44

[4] H. Maesaka et. Al Development of the RF cavity BPM of XFEL/SPRING-8, Proceedings of DIPAC 09, p56

[5] S. Smith et. al. LCLS cavity position monitors, Proceedings of DIPAC 09, p285

[6] W. Bruns, Improved GdfidL with Generalized Diagonal Fillings and Reduced Memory and CPU Requirements, Proceedings of the 1998 International Computational Accelerator Physics Conference (ICAP '98)

[7] S. Y.Lee Accelerator Physics, World scientific publishing, 2004